



The dipole vortex

Henk F. Arnoldus *, John T. Foley

Department of Physics and Astronomy, Mississippi State University, P.O. Drawer 5167, Mississippi State, MS 39762-5167, USA

Received 3 October 2003; accepted 4 December 2003

Abstract

We show that the field lines of the Poynting vector of the radiation field of an electric dipole are vortices if the radiation carries angular momentum. When such a dipole is located near the surface of a perfect conductor, it induces a current density on the surface, and it is shown that the field line pattern of this current density consists of infinite spirals. We have identified a Master Spiral to which all field line spirals converge asymptotically. It is also shown that the field lines of the Poynting vector of the radiation field near the surface contain a vortex.

© 2003 Elsevier B.V. All rights reserved.

PACS: 03.50.De; 42.25.Bs

Keywords: Dipole radiation; Optical vortex; Mirror dipole; Singular circles; Master spiral

1. Introduction

A singular point in an optical radiation field is a point where the amplitude of the field vanishes, and hence the phase in that point is undefined. For a long time, such phase singularities were considered more of a curiosity, until Nye and Berry [1] showed that singular points appear in a radiation field quite naturally, as phase dislocations in traveling waves. A particularly interesting phenomenon is the optical vortex, the center of which is a singular point. Such vortices appear, for instance, in interference patterns between incident waves and diffracted or

reflected waves. The earliest example is the diffraction of a plane wave by a half-infinite screen, where vortices appear at the illuminated side of the screen [2]. More recently, it was found that vortices occur in the diffracted field of a plane wave by a slit in a screen [3,4], and in interference between three plane waves [5]. Another example is the field structure in the focal plane of a focusing lens, where the energy flow exhibits vortex lines [6,7]. It seems that optical vortices which appear in the field of a Laguerre–Gaussian (laser) beam are the most widely studied [8–11].

In an optical vortex, the field lines of the Poynting vector, representing the energy flow, circulate around the singular point (two dimensions) or around a vortex axis (three dimensions). There seems to be an intimate relation between the angular momentum of the light [12–15], and the

* Corresponding author. Tel.: +1-662-325-2919; fax: +1-662-325-8898.

E-mail addresses: arnoldus@ra.msstate.edu (H.F. Arnoldus), jtfl@ra.msstate.edu (J.T. Foley).

existence of vortices in the radiation field. Although this relation is not clear in general, it is well established that for the Laguerre–Gaussian beam vortices are only observed for modes that carry angular momentum [16,17]. Conversely, if a radiation field carries angular momentum, one would expect that there is a possibility that vortices are present. In this paper we shall show that for the field of the simplest and most important radiating system, the electric dipole, the appearance of a vortex and the presence of angular momentum in the field go hand-in-hand.

2. Dipole radiation

We consider an electric dipole moment $\mathbf{d}(t)$, with complex amplitude \mathbf{d} and oscillating harmonically with angular frequency ω :

$$\mathbf{d}(t) = \text{Re}[\mathbf{d}e^{-i\omega t}]. \quad (1)$$

The electric field, emitted by the dipole, is written as

$$\mathbf{E}(\mathbf{r}, t) = \text{Re}[\mathbf{E}(\mathbf{r})e^{-i\omega t}], \quad (2)$$

and when the dipole is located at the origin of coordinates, the complex amplitude $\mathbf{E}(\mathbf{r})$ is given by [18]

$$\mathbf{E}(\mathbf{r}) = \frac{k^3}{4\pi\epsilon_0 q} \left\{ \mathbf{d} - (\mathbf{d} \cdot \hat{\mathbf{r}})\hat{\mathbf{r}} + \frac{1}{q} \left(\frac{1}{q} - i \right) [3(\mathbf{d} \cdot \hat{\mathbf{r}})\hat{\mathbf{r}} - \mathbf{d}] \right\} e^{iq}, \quad (3)$$

with $k = \omega/c$. The dimensionless radial distance between the dipole and the field point \mathbf{r} is $q = kr$, and $\hat{\mathbf{r}}$ is the radial unit vector. The corresponding magnetic field is

$$\mathbf{B}(\mathbf{r}, t) = \text{Re}[\mathbf{B}(\mathbf{r})e^{-i\omega t}], \quad (4)$$

with complex amplitude

$$\mathbf{B}(\mathbf{r}) = \frac{1}{c} \frac{k^3}{4\pi\epsilon_0 q} \left(1 + \frac{i}{q} \right) (\hat{\mathbf{r}} \times \mathbf{d}) e^{iq}. \quad (5)$$

3. Poynting vector and emitted power

The Poynting vector is defined as $\mathbf{S}(\mathbf{r}, t) = \mathbf{E}(\mathbf{r}, t) \times \mathbf{B}(\mathbf{r}, t)/\mu_0$ in terms of the time dependent fields. With Eqs. (2) and (4) we can express this in

terms of the complex amplitudes of the electric and magnetic fields as

$$\mathbf{S}(\mathbf{r}) = \frac{1}{2\mu_0} \text{Re}[\mathbf{E}(\mathbf{r}) \times \mathbf{B}(\mathbf{r})^*], \quad (6)$$

where we have dropped terms that oscillate at twice the optical frequency. For time harmonic fields, the Poynting vector is time independent, so we write $\mathbf{S}(\mathbf{r})$ instead of $\mathbf{S}(\mathbf{r}, t)$. We then substitute the right-hand sides of Eqs. (3) and (5), and work out the cross product. This yields

$$\mathbf{S}(\mathbf{r}) = \frac{ck^6}{32\pi^2\epsilon_0 q^2} \left\{ [\mathbf{d} \cdot \mathbf{d}^* - (\mathbf{d} \cdot \hat{\mathbf{r}})(\mathbf{d}^* \cdot \hat{\mathbf{r}})]\hat{\mathbf{r}} - \frac{2}{q} \left(1 + \frac{1}{q^2} \right) \text{Im}[(\mathbf{d} \cdot \hat{\mathbf{r}})\mathbf{d}^*] \right\}. \quad (7)$$

The significance of the Poynting vector is that $\hat{\mathbf{n}} \cdot \mathbf{S}(\mathbf{r}) dA$, with $\hat{\mathbf{n}}$ a unit vector perpendicular to the surface element dA represents the energy per unit of time flowing through dA into the direction of $\hat{\mathbf{n}}$. We now consider a sphere with radius R , and centered at the origin. We then have $\hat{\mathbf{n}} = \hat{\mathbf{r}}$, which gives $\text{Im}[(\mathbf{d} \cdot \hat{\mathbf{r}})\mathbf{d}^*] \cdot \hat{\mathbf{r}} = 0$, showing that the second term in braces in Eq. (7) does not contribute to the radial power flow. Since $q = kR$ on the sphere and $dA = R^2 \sin\theta d\theta d\phi$ in spherical coordinates, we see that $\hat{\mathbf{r}} \cdot \mathbf{S}(\mathbf{r}) dA$ is independent of R . We then obtain for the emitted power by the dipole

$$\frac{dU_{\text{em}}}{dt} = \oint \hat{\mathbf{r}} \cdot \mathbf{S}(\mathbf{r}) dA = \omega \frac{k^3}{12\pi\epsilon_0} \mathbf{d}^* \cdot \mathbf{d}, \quad (8)$$

a well-known result [19], which is usually derived by only considering the fields for R large (far field).

4. Spherical unit vectors

The Poynting vector $\mathbf{S}(\mathbf{r})$, Eq. (7), has a radial part, proportional to $\hat{\mathbf{r}}$, and a part that depends on the orientation of the complex amplitude \mathbf{d} of the dipole. We shall now assume that \mathbf{d} is proportional to a spherical unit vector

$$\mathbf{d} = d_0 e^{i\psi} \mathbf{e}_\tau, \quad \tau = -1, 0, 1, \quad (9)$$

with $d_0 > 0$ and ψ an overall phase. When the dipole is an atom, the emitted radiation is fluorescence and the dipole moment has the form as in Eq. (9). For $\tau = 0$ we have a $\Delta m = 0$ transition and $\tau = \pm 1$ corresponds to a $\Delta m = 1$ transition. The

helicity τ refers to a preferred direction, taken to be the z -axis, and for a quantum field this is the quantization axis. For $\tau = 0$ we have $\mathbf{e}_0 = \mathbf{e}_z$, and with Eq. (1) this gives for the dipole moment $\mathbf{d}(t) = d_0 \mathbf{e}_z \cos(\omega t - \psi)$, representing a linear dipole directed along the z -axis.

For $\tau = \pm 1$ the unit vectors are defined as

$$\mathbf{e}_{\pm 1} = \frac{1}{\sqrt{2}}(\mp \mathbf{e}_x - i \mathbf{e}_y), \quad (10)$$

and the corresponding dipole moment is

$$\mathbf{d}(t) = \frac{d_0}{\sqrt{2}}[\mp \mathbf{e}_x \cos(\omega t - \psi) - \mathbf{e}_y \sin(\omega t - \psi)]. \quad (11)$$

For $\tau = 1$ the dipole moment rotates counter-clockwise (from $+x$ to $+y$) in the xy -plane, and for $\tau = -1$ the rotation is clockwise.

The spherical unit vectors are normalized as $\mathbf{e}_\tau^* \cdot \mathbf{e}_\tau = 1$, and therefore we have $\mathbf{d}^* \cdot \mathbf{d} = d_0^2$. For the emitted power, Eq. (8), we shall write P_0 , which is

$$P_0 = \omega \frac{k^3 d_0^2}{12\pi\epsilon_0}. \quad (12)$$

Furthermore, it follows by inspection that

$$-2\text{Im}[(\mathbf{e}_\tau \cdot \hat{\mathbf{r}})\mathbf{e}_\tau^*] = \tau \mathbf{e}_\phi \sin \theta \quad (13)$$

in spherical coordinates, and therefore the Poynting vector becomes

$$\mathbf{S}(\mathbf{r}) = \frac{3k^2 P_0}{8\pi q^2} \left\{ [1 - (\mathbf{e}_\tau \cdot \hat{\mathbf{r}})(\mathbf{e}_\tau^* \cdot \hat{\mathbf{r}})] \hat{\mathbf{r}} + \frac{\tau}{q} \left(1 + \frac{1}{q^2}\right) \sin \theta \mathbf{e}_\phi \right\}. \quad (14)$$

The radial part can be simplified as

$$1 - (\mathbf{e}_\tau \cdot \hat{\mathbf{r}})(\mathbf{e}_\tau^* \cdot \hat{\mathbf{r}}) = \begin{cases} \sin^2 \theta, & \tau = 0, \\ 1 - \frac{1}{2} \sin^2 \theta, & \tau = \pm 1. \end{cases} \quad (15)$$

5. Field lines of the Poynting vector

For a dipole with a dipole moment along the z -axis, the Poynting vector is given by Eq. (14) with $\tau = 0$

$$\mathbf{S}(\mathbf{r}) = \frac{3k^2 P_0}{8\pi q^2} \sin^2 \theta \hat{\mathbf{r}}. \quad (16)$$

At any field point, $\mathbf{S}(\mathbf{r})$ is proportional to $\hat{\mathbf{r}}$, with the constant of proportionality positive. Therefore, the field lines are straight lines, starting at the origin and radially outward.

More interesting is the case of a rotating dipole moment in the xy -plane. The field lines of the vector field $\mathbf{S}(\mathbf{r})$ are curves $\mathbf{r}(u)$, with u a dummy parameter, for which at each point of the curve, $\mathbf{S}(\mathbf{r})$ is the tangent vector of the curve. Therefore, the field lines are the solutions of

$$\frac{d\mathbf{r}}{du} = \mathbf{S}(\mathbf{r}). \quad (17)$$

In spherical coordinates this is equivalent to the following set of three coupled differential equations for the coordinates r , θ and ϕ as a function of u :

$$\frac{dr}{du} = \mathbf{S}(\mathbf{r}) \cdot \hat{\mathbf{r}}, \quad (18)$$

$$r \frac{d\theta}{du} = \mathbf{S}(\mathbf{r}) \cdot \mathbf{e}_\theta, \quad (19)$$

$$r \sin \theta \frac{d\phi}{du} = \mathbf{S}(\mathbf{r}) \cdot \mathbf{e}_\phi. \quad (20)$$

A great simplification in the computation of field lines arises if one realizes that the vector fields $\mathbf{S}(\mathbf{r})$ and $f(\mathbf{r})\mathbf{S}(\mathbf{r})$, with $f(\mathbf{r})$ an arbitrary positive function of \mathbf{r} , have the same field lines. For instance, if one would take $f(\mathbf{r}) = 1/|\mathbf{S}(\mathbf{r})|$, then the parameter u equals the arc length of the field line. For the problem at hand, we take $f(\mathbf{r})$ as

$$f(\mathbf{r}) = \left[\frac{3k^3 P_0}{8\pi q^2} \left(1 - \frac{1}{2} \sin^2 \theta\right) \right]^{-1}. \quad (21)$$

The set of Eqs. (18)–(20) for the field lines then becomes

$$\frac{dq}{du} = 1, \quad (22)$$

$$\frac{d\theta}{du} = 0, \quad (23)$$

$$\frac{d\phi}{du} = \frac{\tau}{1 - \frac{1}{2} \sin^2 \theta} \frac{1}{q^2} \left(1 + \frac{1}{q^2}\right). \quad (24)$$

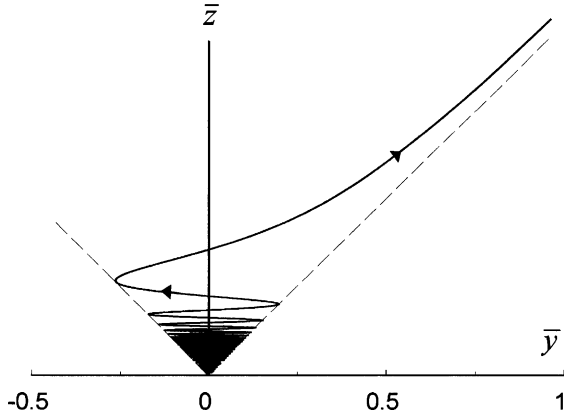


Fig. 1. Field line of the Poynting vector for a dipole with helicity $\tau = 1$, and for $\theta_0 = \pi/4$ and $\phi_0 = \pi/2$. The field line is projected onto the yz -plane, and we use the dimensionless coordinates $\bar{x} = kx$, etc. The field line spirals around the z -axis an infinite number of times and lies on the cone $\theta = \pi/4$, which is indicated by the dashed line. The arrows indicate the direction of the field line. The arrow pointing to the left is behind the z -axis, since the orientation of the field line is counterclockwise with respect to the xy -plane.

From Eq. (22) we see that we can take $u = q$ as the free parameter. The second equation gives $\theta = \theta_0$, e.g., θ is constant on a field line. Since $q > 0$ is the free parameter, we find that a field line starts at the origin and lies on the cone $\theta = \theta_0$. The solution of Eq. (24) is

$$\phi(q) = \phi_0 - \frac{\tau}{1 - \frac{1}{2} \sin^2 \theta_0} \frac{1}{q} \left(1 + \frac{1}{3q^2} \right), \quad (25)$$

with ϕ_0 a constant. We then see that $\phi_0 = \phi(\infty)$, and therefore the two integration constants θ_0 and ϕ_0 are the coordinates θ and ϕ of a point on the field line far from the origin. For $\tau = 1$ the angle $\phi(q)$ increases with q , so that the field line winds around the z -axis in a counterclockwise direction, both for $z > 0$ and for $z < 0$, and stays on the cone $\theta = \theta_0$. The orientation of the field line is the same as the rotation direction of the dipole moment. For $\tau = -1$ the orientation reverses. Fig. 1 illustrates the resulting vortex.

6. Relation to angular momentum

The angular momentum density of an electromagnetic field is given by $\mathfrak{S}(\mathbf{r}, t) = \epsilon_0 \mathbf{r} \times [\mathbf{E}(\mathbf{r}, t)$

$\times \mathbf{B}(\mathbf{r}, t)]$ in terms of the time dependent fields. This density is related in a simple way to the Poynting vector according to

$$\mathfrak{S}(\mathbf{r}) = \epsilon_0 \mu_0 \mathbf{r} \times \mathbf{S}(\mathbf{r}), \quad (26)$$

which is also independent of time, after dropping the terms that oscillate with twice the optical frequency. With Eq. (7) we then immediately obtain

$$\mathfrak{S}(\mathbf{r}) = \frac{1}{c} \frac{k^5}{16\pi^2 \epsilon_0 q^2} \left(1 + \frac{1}{q^2} \right) \text{Im}[(\mathbf{d} \cdot \hat{\mathbf{r}})(\mathbf{d}^* \times \hat{\mathbf{r}})]. \quad (27)$$

Angular momentum is emitted by the dipole, and it is shown in Appendix A that the angular momentum per unit of time passing through a sphere of radius R , centered around the origin, is given by

$$\frac{d\mathbf{J}_{\text{em}}}{dt} = \oint \hat{\mathbf{r}} \cdot M(\mathbf{r}) dA = \frac{k^3}{12\pi\epsilon_0} \text{Im}(\mathbf{d}^* \times \mathbf{d}), \quad (28)$$

which is independent of the radius of the sphere. Here, $M(\mathbf{r})$ is the angular momentum flux tensor. This result has a striking resemblance with Eq. (8) for the emitted power. The contribution to the density $\mathfrak{S}(\mathbf{r}, t)$ came from the term containing $\text{Im}[(\mathbf{d} \cdot \hat{\mathbf{r}})\mathbf{d}^*]$ in Eq. (7), and this term gave the tangential (\mathbf{e}_ϕ) component of the Poynting vector, which leads to the vortex. We therefore conclude that the field of a dipole contains a vortex if and only if the angular momentum density of the field is non-zero. Furthermore, $\text{Im}[(\mathbf{d} \cdot \hat{\mathbf{r}})\mathbf{d}^*]$ can only be non-zero if the dipole moment \mathbf{d} has an imaginary part, which is also a necessary condition for a non-zero emission rate, since $\text{Im}(\mathbf{d}^* \times \mathbf{d})$ is zero for \mathbf{d} real.

For a dipole moment of the form (9) we have

$$\text{Im}(\mathbf{d}^* \times \mathbf{d}) = \tau d_0^2 \mathbf{e}_z, \quad (29)$$

which gives for the emission rate

$$\frac{d\mathbf{J}_{\text{em}}}{dt} = \tau \frac{P_0}{\omega} \mathbf{e}_z. \quad (30)$$

This shows that for a linear dipole the emission rate is zero, and for a circular dipole the emission rate is P_0/ω , in either the positive or negative z -direction. For the angular momentum density we have

$$\text{Im}[(\mathbf{d} \cdot \hat{\mathbf{r}})(\mathbf{d}^* \times \hat{\mathbf{r}})] = -\frac{1}{2} \tau d_0^2 \sin \theta \mathbf{e}_\theta, \quad (31)$$

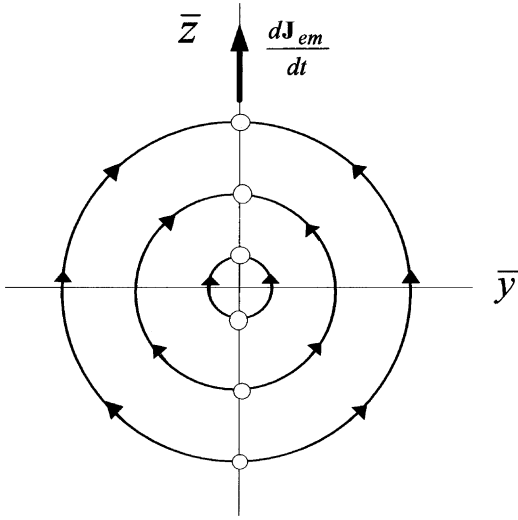


Fig. 2. Illustration of the angular momentum density field lines for a rotating dipole moment in the xy -plane with positive helicity. The lines are semi-circles, starting on the negative z -axis and ending on the positive z -axis. Therefore, the z -axis is a singular line. The total emitted angular momentum is in the positive z -direction.

so that

$$\mathfrak{J}(\mathbf{r}) = -\frac{\tau}{c} \frac{k^5 d_0^2}{32\pi^2 \epsilon_0 q^2} \left(1 + \frac{1}{q^2}\right) \sin \theta \mathbf{e}_\theta. \quad (32)$$

This density is in the \mathbf{e}_θ direction for all \mathbf{r} , and therefore the field lines are the meridians on a sphere. For $\theta = 0$ and $\theta = \pi$, the overall factor $\sin \theta$ on the right-hand side of Eq. (32) makes the density vanish on the z -axis. Consequently, the field lines run from pole to pole on a sphere, which makes the z -axis a singular line. Fig. 2 shows the field lines of the angular momentum density for $\tau = 1$. It is interesting to notice that angular momentum is emitted, with the vector sum being in the z -direction, even though the field lines of the density have no component in the radially outward direction.

7. Dipole near a perfect conductor

When the dipole is located in the vicinity of a perfect conductor, it will induce a surface charge density and a surface current density. We consider

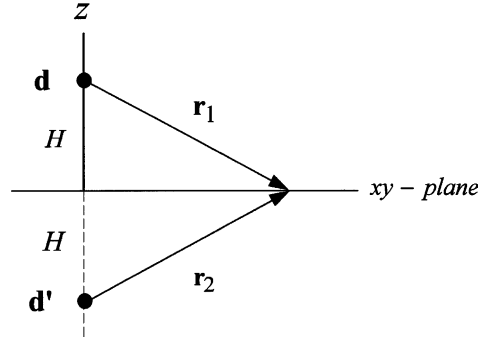


Fig. 3. Schematic setup of the dipole near a perfect conductor. The vectors \mathbf{r}_1 and \mathbf{r}_2 represent the field point \mathbf{r} in the xy -plane, with respect to the dipole and the image dipole, respectively.

the situation shown in Fig. 3. The metal occupies the half-space $z < 0$, and the dipole is located on the z -axis, a distance H above the surface. The field in $z > 0$ is then the sum of the field of the dipole and its mirror image. When we write the dipole moment as $\mathbf{d} = \mathbf{d}_\perp + \mathbf{d}_\parallel$, where the subscripts indicate the perpendicular and parallel parts of \mathbf{d} with respect to the surface, then the image dipole has dipole moment

$$\mathbf{d}' = \mathbf{d}_\perp - \mathbf{d}_\parallel \quad (33)$$

and is located a distance H under the surface. Since there is no field in the half-space $z < 0$, it follows from the boundary conditions at $z = 0$ that the complex amplitude of the induced current density is given by [20]

$$\mathbf{i}(\mathbf{r}) = \frac{1}{\mu_0} \mathbf{e}_z \times \mathbf{B}(\mathbf{r}), \quad (34)$$

with $\mathbf{B}(\mathbf{r})$ the field just above the xy -plane, and the time dependent current density is

$$\mathbf{i}(\mathbf{r}, t) = \text{Re}[\mathbf{i}(\mathbf{r})e^{-i\omega t}]. \quad (35)$$

The current density does not have fast oscillating terms that would have to be dropped.

The magnetic field for a dipole at the origin of coordinates is given by Eq. (5). We replace \mathbf{r} by \mathbf{r}_1 for the field of the dipole and by \mathbf{r}_2 for the field of the image dipole. For a point in the xy -plane we have $r_1 = r_2$, and we shall use the dimensionless variable

$$q_1 = kr_1 \quad (36)$$

for the distance between the dipole and the field point in the xy -plane. The magnetic field near the xy -plane then becomes

$$\mathbf{B}(\mathbf{r}) = \frac{k^4}{4\pi\epsilon_0cq_1^2} \left(1 + \frac{i}{q_1}\right) (\mathbf{r}_1 \times \mathbf{d} + \mathbf{r}_2 \times \mathbf{d}') \mathbf{e}^{iq_1}. \tag{37}$$

With the definition (33) of the mirror dipole and the relations between the various vectors in Fig. 3 ($\mathbf{r}_1 = \mathbf{r} - H\mathbf{e}_z$, etc.) this can be written as

$$\mathbf{B}(\mathbf{r}) = \frac{-k^4}{2\pi\epsilon_0cq_1^2} \left(1 + \frac{i}{q_1}\right) \mathbf{e}^{iq_1} \mathbf{e}_z \times (d_z\mathbf{r} + H\mathbf{d}_{\parallel}). \tag{38}$$

For the current density we then obtain

$$\mathbf{i}(\mathbf{r}, t) = \frac{ck^3}{2\pi q_1^2} \text{Re} \left[\left(1 + \frac{i}{q_1}\right) \mathbf{e}^{i(q_1 - \omega t)} (d_z q_1 \hat{\mathbf{r}} + h\mathbf{d}_{\parallel}) \right], \tag{39}$$

where $q = kr$ as before, and we have also set $h = kH$ for the dimensionless distance between the dipole and the surface.

8. Linear dipole moment

Let us first consider a linear dipole oriented along the z -axis, for which the dipole moment is given by Eq. (9) with $\tau = 0$. Then the current density (39) simplifies to

$$\mathbf{i}(\mathbf{r}, t) = \frac{i_0}{q_1^2} q \left[\cos(q_1 - \alpha) - \frac{1}{q_1} \sin(q_1 - \alpha) \right] \hat{\mathbf{r}}, \tag{40}$$

with

$$i_0 = \frac{ck^3 d_0}{2\pi}, \tag{41}$$

and for the time parameter we introduce the dimensionless abbreviation

$$\alpha = \omega t - \psi. \tag{42}$$

The field lines of the current density are in the radial direction, and they can be inward or outward, depending on the sign of the factor in square brackets. This also implies that the current density is zero if the term in square brackets vanishes, e.g., if

$$\tan(q_1 - \alpha) = q_1, \tag{43}$$

with

$$q_1 = \sqrt{q^2 + h^2}. \tag{44}$$

For a given α (or time), Eq. (43) has an infinite number of solutions q . Each q corresponds to a circle in the xy -plane on which the current density is zero, and hence these are singular circles. When going across a singular circle in the radial direction, the term in square brackets in Eq. (40) changes sign, and therefore the current density changes direction. This leads to the field line picture shown in Fig. 4 for a fixed value of α . For $q \gg 1, h$, the term in square brackets reduces to approximately $\cos(q - \alpha)$, and this term vanishes in intervals of π , given α . Therefore, for q large, the separation between the circles in Fig. 4 becomes approximately half a wavelength. Furthermore, we notice that $\mathbf{i}(\mathbf{r}, t)$ has an overall factor of q , which makes the origin of coordinates a singular point.

We now consider the change in the field line picture when time progresses. First of all, when we consider a fixed point \mathbf{r} , the current density oscillates harmonically in the radial direction. On the other hand, when we replace α by $\alpha + 2\pi$ in Eq. (40), the current density remains unchanged.

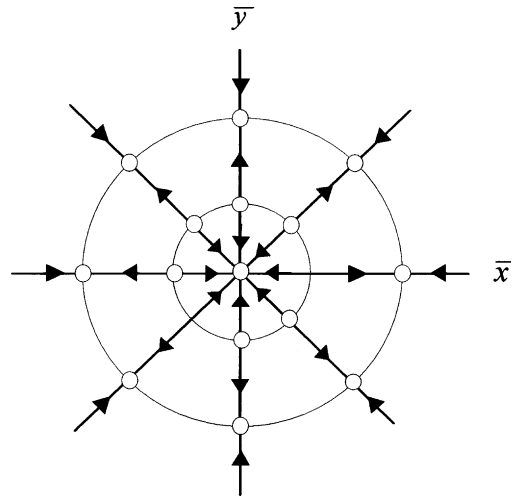


Fig. 4. Field line pattern of the current density in the xy -plane for the case of a dipole oriented perpendicular to the surface, and for a fixed time. The circles are singular circles on which the current density is zero, and they expand with a speed given by Eq. (45) when time progresses. The origin of coordinates is a singular point.

Therefore, the picture repeats itself every $\Delta t = 2\pi/\omega$. Let us now consider the time evolution of the singular circles. For a given α , Eq. (43) determines a series of values of q , each representing a singular circle. For varying α , we can see this as a set of functions $q(\alpha)$. The rate of change with α of the solutions $q(\alpha)$ is $dq/d\alpha$, which can be found by differentiating Eq. (43) with respect to α . With $q = kr$ and $\alpha = \omega t - \psi$ we have $dr/dt = (\omega/k)dq/d\alpha$, and $\omega/k = c$, the speed of light. We then find for the rate of change of the radii of the circles

$$v = \frac{dr}{dt} = c\sqrt{1 + (h/q)^2} + \frac{c}{q^2\sqrt{1 + (h/q)^2}}. \quad (45)$$

In other words, a singular circle with radius r expands in time with this radial velocity v . It is interesting to see that this velocity depends on q , and that v is larger than the speed of light. For $q = 0$ we have $v = \infty$ and for $q \rightarrow \infty$, we have $v \rightarrow c$. The reason why different circles expand at a different speed is the following. Every $\Delta t = 2\pi/\omega$ the field line picture reproduces itself. Say we start at $t = 0$. Then, in a time Δt a circle must expand at such a rate that it ends up exactly at the location where the second next singular circle was at $t = 0$. But since the circles are not evenly spaced, the distance traveled in time Δt differs from circle to circle.

Next we consider a dipole oriented parallel to the surface of the perfect conductor, say in the x -direction. The current density then becomes

$$\mathbf{i}(\mathbf{r}, t) = \frac{i_0}{q_1^2} h \left[\cos(q_1 - \alpha) - \frac{1}{q_1} \sin(q_1 - \alpha) \right] \mathbf{e}_x. \quad (46)$$

The current density is now in the x -direction for all field points. The term in square brackets is the same as in Eq. (40), so this current distribution has the same singular circles as for the perpendicular dipole. As compared to Eq. (40), here we have an overall factor h , rather than q , and therefore the origin of coordinates is not a singular point for this case. Fig. 5 shows the field line pattern for the parallel dipole.

Finally, let us consider the case of a linear dipole moment with arbitrary orientation. We then have $\mathbf{d} = d_0 \exp(i\psi)\mathbf{u}$, with \mathbf{u} real, and the time

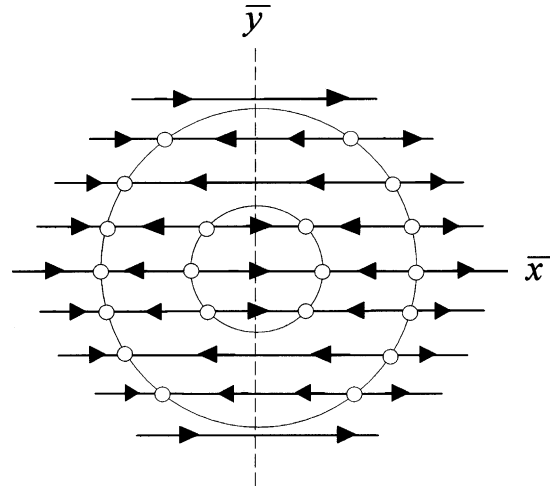


Fig. 5. Field lines of the current density in the surface of the conductor for a dipole in the x -direction.

dependent dipole moment is $\mathbf{d}(t) = d_0 \cos(\omega t - \psi)\mathbf{u}$. The current density becomes

$$\mathbf{i}(\mathbf{r}, t) = \frac{i_0}{q_1^2} q \left[\cos(q_1 - \alpha) - \frac{1}{q_1} \sin(q_1 - \alpha) \right] \times \left(u_z \hat{\mathbf{r}} + \frac{h}{q} \mathbf{u}_{\parallel} \right). \quad (47)$$

As compared to Eq. (40) we see that the $\hat{\mathbf{r}}$ component is multiplied by u_z , and that a term $(h/q)\mathbf{u}_{\parallel}$ adds to the radial part. For $q \gg h$ this second term is negligible, and the field lines are the same as in Fig. 4. Only near the origin will there be a contribution from the parallel component of the dipole moment. Therefore, the general field line picture of the current density is as in Fig. 4, except that near the origin the field lines acquire a component proportional to \mathbf{u}_{\parallel} . As a consequence, the origin is not a singular point anymore. This also means that a field line pattern as in Fig. 5 can only occur if the dipole moment is exactly parallel to the xy -plane. The slightest contribution from a z -component will dominate the field pattern for q large.

9. Rotating dipole moment

We now consider a rotating dipole moment, parallel to the xy -plane, and we shall take \mathbf{d} as in Eq. (9) with $\tau = 1$. When we substitute this

expression for \mathbf{d} into Eq. (39), we find for the current density an expression similar to Eq. (47) for the linear dipole moment. For the discussion in this and the following sections it is advantageous to combine the sin and cos terms in the square brackets, which yields

$$\mathbf{i}(\mathbf{r}, t) = \frac{i_0 h}{q_1^2 \sqrt{2}} \sqrt{1 + \frac{1}{q_1^2}} [\sin(q_1 - \delta - \alpha) \mathbf{e}_x + \cos(q_1 - \delta - \alpha) \mathbf{e}_y], \quad (48)$$

with

$$\delta = \arctan(q_1). \quad (49)$$

For a fixed point in the xy -plane, the magnitude of the current density is the same for all time t (all α), since the vector in square brackets in Eq. (48) is a unit vector. When time progresses, this vector rotates with angular frequency ω in the counterclockwise direction. Therefore, at each point in the xy -plane, $\mathbf{i}(\mathbf{r}, t)$ is a rotating vector of constant magnitude. Furthermore, for a given value of q , e.g., on a circle around the origin, the current density is the same in magnitude and direction at any point on this circle. Therefore, vectors $\mathbf{i}(\mathbf{r}, t)$ on a circle all point in the same direction and they each rotate counterclockwise with angular frequency ω . This gives rise to a very peculiar field line pattern, as we shall show below.

For the field lines we shall use the dimensionless Cartesian coordinates $\bar{x} = kx$ and $\bar{y} = ky$. Points on a field line have coordinates (\bar{x}, \bar{y}) , which are parameterized with the dummy variable u , and these functions $\bar{x}(u)$ and $\bar{y}(u)$ are the solutions of

$$\frac{d\bar{x}}{du} = \sin(q_1 - \delta - \alpha), \quad (50)$$

$$\frac{d\bar{y}}{du} = \cos(q_1 - \delta - \alpha), \quad (51)$$

with

$$q_1 = \sqrt{\bar{x}^2 + \bar{y}^2 + h^2}, \quad (52)$$

and δ given by Eq. (49). A field line goes through each point in the xy -plane, and the choice of any such point, say (\bar{x}_0, \bar{y}_0) , determines the solution of this set of equations. It does not appear possible to solve this set analytically, so we shall resort to nu-

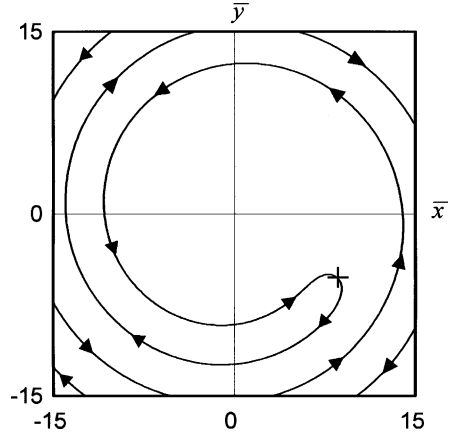


Fig. 6. Typical field line for the current density in the xy -plane, induced by a counterclockwise rotating dipole moment for $\alpha = 0$ and $h = 1$. The given point on the field line is $(\bar{x}_0, \bar{y}_0) = (8, -5)$, and this point is indicated by +.

merical integration. We use fourth-order Runge-Kutta integration [21].

Fig. 6 shows a typical field line through a given point (\bar{x}_0, \bar{y}_0) . Near this given point, the field line turns rapidly, and then it spirals out in the clockwise direction when integrated forward (du positive in Eqs. (50) and (51)). If we integrate backwards, it also spirals out. Since this is integrated against the field line, this is a field line that spirals inwards and ends up exactly at the given point (\bar{x}_0, \bar{y}_0) . These spirals continue indefinitely, and fill up the entire xy -plane. It is interesting to see that the incoming spiral lies in between the outgoing spiral and runs in the opposite direction. Exactly at the given point (\bar{x}_0, \bar{y}_0) the incoming counterclockwise spiral reverses direction and continues as the outgoing clockwise spiral. There is nothing special about the point (\bar{x}_0, \bar{y}_0) for Fig. 6; field lines through any point show similar behavior. Since we know that field lines of any vector field cannot cross, and since we already fill up the entire xy -plane with the field line through a single given point, it is not obvious what the general field line picture looks like.

10. The Master Spiral

We now introduce a set of two curves, defined in polar coordinates (q, ϕ) by

$$\phi(q) = \delta - q_1 + \alpha + n\pi, \quad n = 0, 1, \quad (53)$$

where δ and q_1 are functions of q , and h and α are constants. For each value of q , with $0 \leq q < \infty$, the dimensionless Cartesian coordinates of the corresponding point in the xy -plane then follow from

$$\bar{x} = q \cos \phi, \quad \bar{y} = q \sin \phi. \quad (54)$$

If (\bar{x}, \bar{y}) is a point on the curve with $n = 0$ for a given q , then it follows immediately that for the same q the point on the curve with $n = 1$ is $(-\bar{x}, -\bar{y})$. Since both curves are defined for $q = 0$, they connect at the origin.

On a curve, $\alpha + n\pi$ is constant. If we follow the $n = 0$ curve, and q increases by an amount such that $\delta - q_1$ decreases by exactly 2π , then the curve makes a full rotation around the origin in the clockwise direction because ϕ decreases by 2π . Since over this full rotation q increases, the curve does not close on itself. If we keep on increasing q , the curve keeps on spiraling around the origin, up to infinity. The curve with $n = 1$ has the same appearance, and a moment of thought shows that this spiral runs in between the $n = 0$ spiral (consider a point (\bar{x}, \bar{y}) on the $n = 0$ spiral and the corresponding point $(-\bar{x}, -\bar{y})$ on the $n = 1$ spiral; then decrease ϕ for both simultaneously). We now assign an orientation to these curves. The $n = 0$ curve is defined to run into the direction of increasing ϕ , so that it spirals inward from infinity in the counterclockwise direction. The $n = 1$ spiral is given an orientation such that it runs into the direction of decreasing ϕ , and therefore it spirals outward from the origin, in between the first spiral, and in the clockwise direction. Since the curves connect at the origin, we effectively have one curve, which is shown in Fig. 7. We call this the *Master Spiral*, for reasons explained below.

From Eq. (53) we obtain

$$\frac{d\phi}{dq} = -\frac{qq_1}{1 + q_1^2}, \quad (55)$$

and with Eq. (54) we then derive

$$\frac{d\bar{y}}{d\bar{x}} = \frac{(1 + q_1^2) \sin \phi - q^2 q_1 \cos \phi}{(1 + q_1^2) \cos \phi + q^2 q_1 \sin \phi} \quad (56)$$

for the slope of the curve in any given point. In particular, at the origin of coordinates this be-

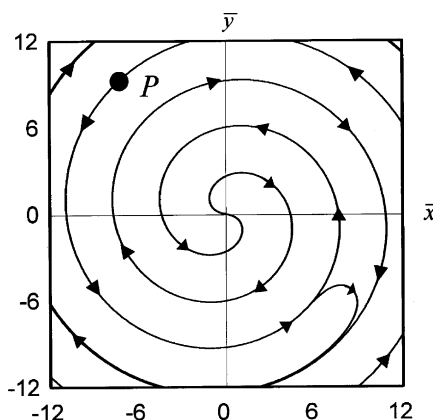


Fig. 7. Graph of the Master Spiral for $\alpha = 0$ and $h = 1$. When we start at point P , which is on the $n = 0$ curve, the curve spirals inward in the counterclockwise direction, until it reaches the origin of coordinates. It then continues to spiral outward as the $n = 1$ curve in the clockwise direction. Also shown is the field line from Fig. 6.

comes $\tan \phi$, and with $q_1 = h$ and Eq. (53) this gives

$$\frac{d\bar{y}}{d\bar{x}} = -\tan(h - \delta - \alpha), \quad (57)$$

both for the $n = 0$ and the $n = 1$ curve. Therefore, they connect smoothly. Furthermore, we see from Eq. (55) that $dq/d\phi \rightarrow -1$ for q large, so that $q \approx -\phi + \text{constant}$, and therefore the radius of a loop of the spiral increases by 2π in dimensionless units in each rotation, which corresponds to one wavelength.

11. The field line pattern

We now return to the problem of the field lines of the current density for the case of the rotating dipole moment. We change Eq. (48) to polar coordinates, which gives

$$\mathbf{i}(\mathbf{r}, t) = \frac{i_0 h}{q_1^2 \sqrt{2}} \sqrt{1 + \frac{1}{q_1^2}} [\sin(q_1 - \delta + \phi - \alpha) \hat{\mathbf{r}} + \cos(q_1 - \delta + \phi - \alpha) \mathbf{e}_\phi], \quad (58)$$

and the equations for the field lines, Eqs. (50) and (51), transform into

$$\frac{dq}{du} = \sin(q_1 - \delta + \phi - \alpha), \quad (59)$$

$$q \frac{d\phi}{du} = \cos(q_1 - \delta + \phi - \alpha). \tag{60}$$

Let us consider a point (q, ϕ) on the Master Spiral, and the field line that goes through this point. From Eq. (53) we see that for every point on the Master Spiral we have

$$\sin(q_1 - \delta + \phi - \alpha) = 0, \tag{61}$$

$$\cos(q_1 - \delta + \phi - \alpha) = (-1)^n. \tag{62}$$

Therefore, the current density simplifies to

$$\mathbf{i}(\mathbf{r}, t) = \frac{i_0 h}{q_1^2 \sqrt{2}} \sqrt{1 + \frac{1}{q_1^2} (-1)^n} \mathbf{e}_\phi. \tag{63}$$

We notice that \mathbf{i} at this point is exactly in the positive ($n = 0$) or negative ($n = 1$) tangential direction, which is the same orientation as the Master Spiral. Furthermore, from Eq. (59) we see that $dq/du \approx 0$ near the Master Spiral, so that when a field line is into the direction of the spiral, it will approximately remain in that direction. Therefore, on or near the Master Spiral, the current density follows the spiral. On the other hand, if we consider a field point in between two loops of the spiral, then we have $\cos(q_1 - \delta + \phi - \alpha) \approx 0$ and $\sin(q_1 - \delta + \phi - \alpha) \approx \pm 1$. From Eq. (58) we then see that \mathbf{i} is approximately in the $\hat{\mathbf{r}}$ direction, either inward or outward. From Eqs. (59) and (60) we furthermore observe that in this area in between the loops of the Master Spiral, q varies rapidly and ϕ is approximately constant. But then, when we follow a field line through a point in between two loops, and q varies significantly, we will approach one of the loops of the spiral. But there \mathbf{i} should be again tangential, and into the direction of the orientation of the spiral. This leads to the conclusion that a field line through a point in between the loops of the spiral rotates quickly, and adjusts itself so as to follow the spiral. This leads to the situation shown in Fig. 6. We have copied that figure into the spiral of Fig. 7, and we see indeed that the field line makes a turn of π , and runs from one loop of the spiral to the adjacent loop, after which it keeps on following the Master Spiral forever. Hence the name Master Spiral.

The reasoning above holds for any point in between the loops of the spiral. The field line picture that emerges is then that there are little lobes everywhere in between the loops of the Master spiral, such as the one shown in Fig. 7. Fig. 8 illustrates the resulting field line pattern. When time progresses, the entire picture rotates with angular velocity ω .

Another way of looking at this is by considering q as a function of ϕ for a field line. From Eqs. (59) and (60) we then have

$$\frac{dq}{d\phi} = q \tan(q_1 - \delta + \phi - \alpha). \tag{64}$$

Far away from the origin we have q large, and this would make $dq/d\phi$ large on a field line, due to the overall factor of q on the right-hand side of Eq. (64). This would imply that q changes rapidly with ϕ , corresponding to a field line that more or less goes out in the radial direction. But such a field line would cross the Master Spiral, and we know that there the field line is exactly in the tangential direction, which is a contradiction. The only possibility is that

$$\tan(q_1 - \delta + \phi - \alpha) \rightarrow 0 \tag{65}$$

for q large, and with $q \tan(q_1 - \delta + \phi - \alpha)$ remaining finite. From Eq. (65) we conclude that $q_1 - \delta + \phi - \alpha \rightarrow 0$ or π for a field line, and this limit is just Eq. (53), defining the Master Spiral.

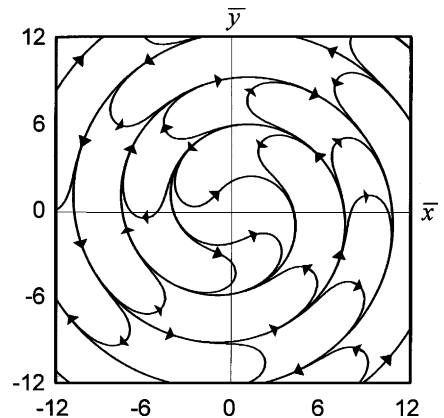


Fig. 8. Illustration of the field line pattern of the current density induced by a rotating dipole moment parallel to the xy -plane, for $\alpha = 0$ and $h = 1$.

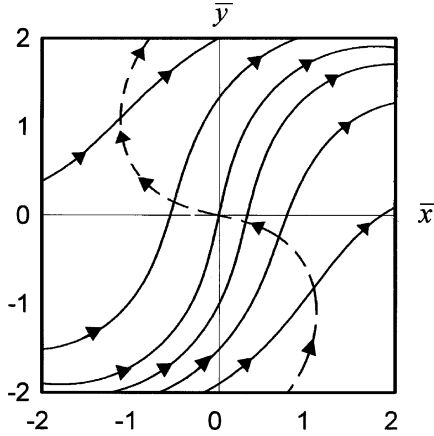


Fig. 9. Enlargement of Fig. 8 to show the field lines of the current density near the origin. The Master Spiral is indicated by the dashed line. We see that the Master Spiral is perpendicular to the field line that goes through the origin of coordinates.

Therefore, any field line approaches the Master Spiral asymptotically.

Near the origin of coordinates, the Master Spiral reverses direction, and the conclusions above might have to be adjusted somewhat. Fig. 9 shows various field lines near the origin, and also shown is the Master Spiral. From the equations for the field lines, Eqs. (50) and (51), we can find the slope $d\bar{y}/d\bar{x}$ of the field lines. At the origin this becomes

$$\frac{d\bar{y}}{d\bar{x}} = \cot(h - \delta - \alpha). \quad (66)$$

Comparison with the slope of the Master Spiral at the origin, Eq. (57), shows that the field line is perpendicular to the spiral at the origin. This also proves that the Master Spiral itself is not a field line, since field lines do not cross. Another interesting feature that can be seen in the graph is that when a field line crosses the Master Spiral, the direction of the field line is still pure tangential, although near the origin that is not the direction of the spiral.

12. Poynting vector in the xy -plane

The electric field at the surface of the perfect conductor is the sum of the field of the dipole and the field of its mirror image. We obtain

$$\mathbf{E}(\mathbf{r}) = \frac{k^3}{2\pi\epsilon_0 q_1} \left\{ -\frac{1}{q_1} \left(\frac{1}{q_1} - i \right) \left[\frac{3h}{q_1} (\mathbf{d} \cdot \hat{\mathbf{r}}_1) + d_z \right] + d_z + \frac{h}{q_1} (\mathbf{d} \cdot \hat{\mathbf{r}}_1) \right\} \mathbf{e}^{iq_1} \mathbf{e}_z, \quad (67)$$

with $\hat{\mathbf{r}}_1$ the unit vector in the \mathbf{r}_1 direction. The magnetic field at the surface is given by Eq. (38), and with Eq. (6) we find for the Poynting vector

$$\mathbf{S}(\mathbf{r}) = \frac{ck^6}{8\pi^2\epsilon_0 q_1^3} \text{Re} \left[(q d_z^* \hat{\mathbf{r}} + h \mathbf{d}_{\parallel}^*) \left(d_z + \frac{h}{q_1} (\mathbf{d} \cdot \hat{\mathbf{r}}_1) + \frac{i}{q_1^2} \left\{ 2h (\mathbf{d} \cdot \hat{\mathbf{r}}_1) + \frac{1}{q_1} \left[\frac{3h}{q_1} (\mathbf{d} \cdot \hat{\mathbf{r}}_1) + d_z \right] \right\} \right) \right]. \quad (68)$$

We shall now consider the same cases as for the current density.

12.1. Real dipole moment

Let the complex amplitude of the dipole moment be given by $\mathbf{d} = d_0 \exp(i\psi) \mathbf{u}$, with \mathbf{u} real. Then the expression for the Poynting vector simplifies considerably

$$\mathbf{S}(\mathbf{r}) = \frac{3k^2 P_0}{2\pi q_1^3} q \left[u_z + \frac{h}{q_1} (\mathbf{u} \cdot \hat{\mathbf{r}}_1) \right] \left(u_z \hat{\mathbf{r}} + \frac{h}{q} \mathbf{u}_{\parallel} \right), \quad (69)$$

with P_0 defined by Eq. (12). The corresponding current density is given by Eq. (47), and we see that the terms in round brackets are the same. Since this factor determines the direction of the vectors $\mathbf{S}(\mathbf{r})$ and $\mathbf{i}(\mathbf{r}, t)$, we find that the Poynting vector and the current density have the same direction, apart from a possible minus sign.

Let us look at $\mathbf{u} = \mathbf{e}_z$, for which the current density is shown in Fig. 4, and given by Eq. (40). With $\mathbf{u} \cdot \hat{\mathbf{r}}_1 = -h/q_1$, the Poynting vector becomes

$$\mathbf{S}(\mathbf{r}) = \frac{3k^2 P_0}{2\pi q_1^5} q^3 \hat{\mathbf{r}}. \quad (70)$$

The field lines are in the radial direction and running outward, with the origin as a singular point ($\mathbf{S}(\mathbf{r}) = 0$ at $q = 0$). The current density, on the other hand, is time dependent and oscillates along the radial direction.

Next we consider $\mathbf{u} = \mathbf{e}_x$, for which the current density is given by Eq. (46) and illustrated in Fig. 5. Now we have $\mathbf{u} \cdot \hat{\mathbf{r}}_1 = (q/q_1) \cos \phi$, and we find for the Poynting vector

$$\mathbf{S}(\mathbf{r}) = \frac{3k^2 P_0}{2\pi q_1^5} h^2 q \cos \phi \mathbf{e}_x. \quad (71)$$

Due to the factor $\cos \phi$, the field lines are in the positive x -direction for $x > 0$ and the negative x -direction for $x < 0$. On the y -axis the Poynting vector is zero, and therefore the y -axis is a singular line. The field lines are shown in Fig. 10.

12.2. Rotating dipole moment

The field lines of the Poynting vector for a rotating dipole moment in free space are vortices with an orientation following the rotation of the dipole moment, as shown in Fig. 1. We now consider the field lines near the surface of the conductor for a rotating dipole moment a distance H above the surface. Vector \mathbf{d} is given by Eq. (9) with $\tau = 1$. We then have $\mathbf{e}_1 \cdot \hat{\mathbf{r}}_1 = -(q/q_1) \exp(i\phi)/\sqrt{2}$ and, after some rearrangements, Eq. (68) becomes

$$\mathbf{S}(\mathbf{r}) = \frac{3k^2 P_0}{4\pi q_1^5} h^2 q \left[\hat{\mathbf{r}} + \frac{1}{q_1} \left(2 + \frac{3}{q_1^2} \right) \mathbf{e}_\phi \right]. \quad (72)$$

The corresponding current density in polar coordinates is given by Eq. (58), and we see that for the case of the rotating dipole moment the current density and the Poynting vector are not propor-

tional. Both have a radial and a tangential component, indicating a spiraling structure. For the Poynting vector we see that both the $\hat{\mathbf{r}}$ and the \mathbf{e}_ϕ component are positive, so the field lines are radially outward, and they spiral in the counter-clockwise direction. At the origin of coordinates we have $\mathbf{S}(\mathbf{r}) = 0$, which makes the origin a singular point of the field lines, and far away from the origin we have $\mathbf{S}(\mathbf{r}) \propto \hat{\mathbf{r}}$. Apparently, for the rotating dipole moment the field lines of the Poynting vector are very different from the field lines of the current density.

The field lines are determined by the direction of $\mathbf{S}(\mathbf{r})$, which is given by the term in square brackets in Eq. (72). The equations for the field lines in polar coordinates are therefore

$$\frac{dq}{du} = 1, \quad (73)$$

$$q \frac{d\phi}{du} = \frac{1}{q_1} \left(2 + \frac{3}{q_1^2} \right). \quad (74)$$

Eq. (73) shows that we can take $u = q$, so that q becomes the independent variable. Then Eq. (74) can be solved analytically, with result

$$\phi(q) = \phi_0 + \frac{3}{q_1 h^2} + \frac{1}{h} \left(1 + \frac{3}{2h^2} \right) \ln \left(\frac{q_1 - h}{q_1 + h} \right). \quad (75)$$

Here ϕ_0 is a constant, which is equal to ϕ for $q \rightarrow \infty$ (just as in Eq. (25) for the dipole vortex). The dimensionless Cartesian coordinates (\bar{x}, \bar{y}) for points on a field line then follow from Eq. (54). Fig. 11 shows the field line of $\mathbf{S}(\mathbf{r})$ for $\phi_0 = 0$ (and $h = 1$). It follows immediately from Eq. (73) that a value of ϕ_0 different from zero, simply rotates the picture over ϕ_0 . Therefore, all field lines are the same, apart from their angular position in the xy -plane. This in contrast to the field lines for the current density with its intricate structure shown in Fig. 8.

Since $\phi(\infty) = \phi_0$, one would expect that the field line approaches the line $\phi = \phi_0$ for q large. For the case of Fig. 11 with $\phi_0 = 0$, this would be the x -axis. It follows from the figure, however, that this is not the case. Consider q large in Eq. (75). We then have

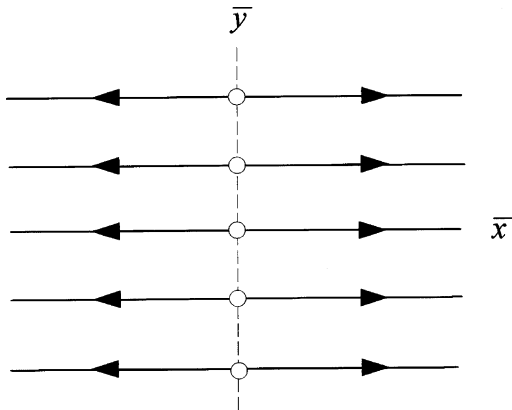


Fig. 10. Field lines of the Poynting vector in the xy -plane for a dipole moment in the x -direction.

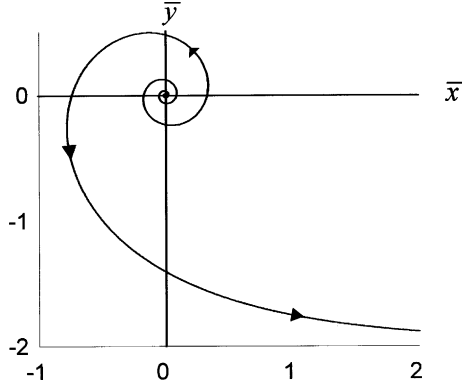


Fig. 11. A field line of the Poynting vector in the xy -plane for a rotating dipole moment parallel to the xy -plane.

$$q_1 \approx q \left(1 + \frac{h^2}{2q^2} \right), \quad (76)$$

which gives

$$\ln \left(\frac{q_1 - h}{q_1 + h} \right) \approx -\frac{2h}{q} \quad (77)$$

and when we then expand the right-hand side of Eq. (75) to lowest order in $1/q$ we obtain

$$\phi \approx \phi_0 - \frac{2}{q}. \quad (78)$$

Remarkably, this is independent of h . Then with Eq. (54) we find the Cartesian coordinates to be

$$\bar{x} \approx q \cos \phi_0 + 2 \sin \phi_0, \quad (79)$$

$$\bar{y} \approx q \sin \phi_0 - 2 \cos \phi_0 \quad (80)$$

for q large. Eqs. (79) and (80) represent a straight line with slope $d\bar{y}/d\bar{x} = \tan \phi_0$, as expected, but the line does not go through the origin of coordinates. For instance, the \bar{y} intercept is $-2/\cos \phi_0$, which is -2 for the case of Fig. 10. Alternatively, for $\phi_0 = 0$, Eq. (80) gives $\bar{y} \approx -2$ for q large.

13. Conclusions

A harmonically oscillating dipole moment emits radiation, and we have shown that the field lines of the Poynting vector are vortices if the radiation carries angular momentum. One of the field lines is shown in Fig. 1 for a dipole

moment that rotates counterclockwise in the xy -plane. When such a rotating dipole moment is placed in the vicinity of a perfect conductor, a current density is induced in the surface. We have studied the field line pattern of this current density, and it was found that each field line consists of two infinite counterrotating spirals that wind into each other, and connect near some point in the xy -plane. We have identified a Master Spiral, which is the asymptotic spiral for all field lines. It was furthermore shown that the field lines of the Poynting vector in the xy -plane are also vortices for the case of a rotating dipole moment in the neighborhood of the xy -plane.

Appendix A

The angular momentum per unit of time passing through a surface element dA into the direction of the unit normal vector $\hat{\mathbf{n}}$ on dA is given by $\hat{\mathbf{n}} \cdot M(\mathbf{r}) dA$, where the angular momentum flux tensor $M(\mathbf{r})$ is defined as [22]

$$M_{ij} = \sum_{k\ell} \varepsilon_{k\ell j} T_{ik} r_\ell. \quad (A.1)$$

The subscripts refer to the Cartesian components of the tensor, and ε is the completely anti-symmetric Lévi-Civita tensor. Here, T is the Maxwell stress tensor, defined as

$$T_{ik} = \varepsilon_0 E_i E_k + \mu_0^{-1} B_i B_k - \delta_{ik} \left(\frac{1}{2} \varepsilon_0 E^2 + \frac{1}{2} \mu_0^{-1} B^2 \right) \quad (A.2)$$

in terms of the time-varying fields. We have $E^2 = \mathbf{E}(\mathbf{r}, t) \cdot \mathbf{E}(\mathbf{r}, t)$. When expressed in terms of the complex amplitude, this becomes $E^2 = (1/2) \mathbf{E}(\mathbf{r}) \cdot \mathbf{E}(\mathbf{r})^*$, with again the fast oscillating terms dropped. With similar expressions for the other terms in Eq. (A.2), the time independent stress tensor becomes

$$T_{ik} = \frac{1}{2} \text{Re}(\varepsilon_0 E_i E_k^* + \mu_0^{-1} B_i B_k^*) - \frac{1}{4} \delta_{ik} (\varepsilon_0 \mathbf{E} \cdot \mathbf{E}^* + \mu_0^{-1} \mathbf{B} \cdot \mathbf{B}^*) \quad (A.3)$$

in terms of the complex amplitudes. When inserted into Eq. (A.1) this yields the time independent angular momentum flux tensor.

For the radial angular momentum flow we have $\hat{\mathbf{n}} = \hat{\mathbf{r}}$, so we need

$$\hat{\mathbf{r}} \cdot \mathbf{M}(\mathbf{r}) = \sum_{ij} \hat{r}_i M_{ij} \mathbf{e}_j, \quad (\text{A.4})$$

and with Eq. (A.1) this is

$$\hat{\mathbf{r}} \cdot \mathbf{M}(\mathbf{r}) = \sum_{ijkl} \hat{r}_i r_\ell \mathbf{e}_j \varepsilon_{k\ell j} T_{ik}. \quad (\text{A.5})$$

Then we insert the right-hand side of Eq. (A.3) and perform the summations. The term with δ_{ik} gives

$$\sum_{ijkl} \hat{r}_i r_\ell \mathbf{e}_j \varepsilon_{k\ell j} \delta_{ik} = \hat{\mathbf{r}} \times \mathbf{r} = 0. \quad (\text{A.6})$$

The term with $E_i E_k^*$ gives

$$\sum_{ijkl} \hat{r}_i r_\ell \mathbf{e}_j \varepsilon_{k\ell j} E_i E_k^* = (\mathbf{E} \cdot \hat{\mathbf{r}})(\mathbf{E}^* \times \mathbf{r}), \quad (\text{A.7})$$

and similarly for the term with $B_i B_k^*$, but since $\mathbf{B} \cdot \hat{\mathbf{r}} = 0$ this term does not contribute. Then we substitute the right-hand side of Eq. (3) for $\mathbf{E}(\mathbf{r})$ which yields

$$\hat{\mathbf{r}} \cdot \mathbf{M}(\mathbf{r}) = -\frac{k^3}{16\pi^2 \varepsilon_0 r^2} \text{Re} \left[\left(\mathbf{i} + \frac{1}{q^3} \right) (\mathbf{d} \cdot \hat{\mathbf{r}})(\mathbf{d}^* \times \hat{\mathbf{r}}) \right]. \quad (\text{A.8})$$

When multiplied by the surface element dA of the sphere, the r -dependence cancels, and integration over the 4π solid angle gives

$$\int d\Omega (\mathbf{d} \cdot \hat{\mathbf{r}})(\mathbf{d}^* \times \hat{\mathbf{r}}) = \frac{4\pi}{3} \mathbf{d}^* \times \mathbf{d}. \quad (\text{A.9})$$

Since $\mathbf{d}^* \times \mathbf{d}$ is pure imaginary, we finally obtain

$$\oint \hat{\mathbf{r}} \cdot \mathbf{M}(\mathbf{r}) dA = \frac{k^3}{12\pi \varepsilon_0} \text{Im}(\mathbf{d}^* \times \mathbf{d}), \quad (\text{A.10})$$

which is Eq. (28). It is interesting to notice that there is no contribution from the magnetic field, and that the contribution to the angular momentum flux comes from combined terms of the far ($1/q$) and middle ($1/q^2$) field. This in contrast to the emitted power, for which only far field terms

contribute, with the electric and magnetic fields both contributing.

References

- [1] J.F. Nye, M.V. Berry, Proc. R. Soc. Lond. A 336 (1974) 165.
- [2] W. Braunbek, G. Laukien, Optik 9 (1952) 174.
- [3] H.F. Schouten, T.D. Visser, G. Gbur, D. Lenstra, H. Blok, Opt. Exp. 11 (2003) 371.
- [4] H.F. Schouten, T.D. Visser, D. Lenstra, H. Blok, Phys. Rev. E 67 (2003) 036608-1-3.
- [5] J. Masajada, B. Dubik, Opt. Commun. 198 (2001) 21.
- [6] B. Richards, E. Wolf, Proc. R. Soc. Lond. A 253 (1959) 358.
- [7] A. Boivin, J. Dow, E. Wolf, J. Opt. Soc. Am. 57 (1967) 1171.
- [8] M. Vasnetsov, K. Staliunas (Eds.), Optical Vortices, Horizons in World Physics, vol. 228, Nova Science, Commack, New York, 1999.
- [9] A.V. Volyar, V.G. Shvedov, T.A. Fadeeva, Opt. Spectrosc. 90 (2001) 93.
- [10] V.A. Pas'co, M.S. Soskin, M.V. Vasnetsov, Opt. Commun. 198 (2001) 49.
- [11] A.V. Volyar, T.A. Fadeeva, V.G. Shvedov, Opt. Spectrosc. 93 (2002) 285.
- [12] L. Allen, M.J. Padgett, M. Babiker, in: E. Wolf (Ed.), Progress in Optics, vol. 39, Elsevier, Amsterdam, 1999, p. 291.
- [13] S.J. van Enk, G. Nienhuis, Opt. Commun. 94 (1992) 147.
- [14] L. Allen, M.W. Beijersbergen, R.J.C. Spreeuw, J.P. Woerdman, Phys. Rev. A 45 (1992) 8185.
- [15] S.J. van Enk, G. Nienhuis, J. Mod. Opt. 41 (1994) 963.
- [16] S.M. Barnett, L. Allen, Opt. Commun. 110 (1994) 670.
- [17] M.S. Soskin, M.V. Vasnetsov, in: E. Wolf (Ed.), Progress in Optics, vol. 42, Elsevier, Amsterdam, 2001, p. 219.
- [18] J.D. Jackson, Classical Electrodynamics, second ed., Wiley, New York, 1975, p. 395.
- [19] P.W. Milonni, J.H. Eberly, Lasers, Wiley, New York, 1988, p. 48.
- [20] J.D. Jackson, Classical Electrodynamics, second ed., Wiley, New York, 1975, p. 20.
- [21] W.H. Press, S.A. Teukolsky, W.T. Vetterling, B.P. Flannery, Numerical Recipes in Fortran 77, second ed., Cambridge University Press, Cambridge, 1992, p. 704.
- [22] S.M. Barnett, J. Opt. B 4 (2002) S7.